Therapeutic Discovery

Molecular Cancer Therapeutics

Inhibition of Monocarboxylate Transporter 2 Induces Senescence-Associated Mitochondrial Dysfunction and Suppresses Progression of Colorectal Malignancies *In Vivo*

Inkyoung Lee[1], Sook-Ja Lee[1], Won Ki Kang[2], and Chaehwa Park[1,2]

Abstract

Senescence, an inherent tumor suppressive mechanism, is a critical determinant for chemotherapy. In the present study, we show that the monocarboxylate transporter 2 (MCT2) protein was tumor-selectively expressed in human colorectal malignancies and knockdown of MCT2 induces mitochondrial dysfunction, cell-cycle arrest, and senescence without additional cellular stress in colorectal cancer cell lines. Moreover, the reactive oxygen species (ROS) scavenger, N-acetylcysteine, blocked MCT2 knockdown-induced growth arrest and cellular senescence, indicating a pivotal role of ROS in this pathway. Dramatic induction of mitochondrial superoxide generation and decrease in ATP production was observed, indicating that mitochondrial dysfunction is the major mechanism underlying MCT2 knockdown-induced ROS generation. Senescence-associated DNA damage was also evident from the increase in promyelocytic leukemia bodies, γH2AX foci, and SAHF. Conversely, overexpression of MCT2 prevented doxorubicin-induced ROS accumulation ($P = 0.0002$) and cell growth inhibition ($P = 0.001$). MCT2 knockdown suppressed KRAS mutant colorectal tumor growth *in vivo*. In addition, MCT2 knockdown and cytostatic drug combination further enhanced the antitumor effect. These findings support the use of MCT2 as a promising target for inhibition of colorectal cancer. *Mol Cancer Ther; 11(11); 2342–51. ©2012 AACR.*

Introduction

Tumors are usually limited in terms of oxygen availability (1) and adapt to hypoxia by uncoupling their glycolytic metabolism from aerobic respiration (2). Persistence of glycolysis, the Warburg effect, is a typical characteristic of advanced cancers. Glycolysis, which produces only 2 ATPs for a glucose molecule, is considered a less effective pathway than aerobic respiration that generates 38 ATP molecules. However, lactic acid released by glucose-consuming hypoxic tumors (2) is consumed as a predominant source of oxidative metabolism of tumor cells (3). The gatekeepers of this metabolic process are monocarboxylate transporters (MCT; MCT1, 2, 3, and 4), which transport monocarboxylates, including pyruvate and lactate (4).

The MCT family comprises 14 members, among which only the first 4 (MCT1–4) catalyze the proton-linked transport of metabolically important monocarboxylates, such as lactate, pyruvate, and ketone bodies (5). MCT2 displays 10-fold higher affinity for monocarboxylates than the MCT1 and MCT4 uptake mechanisms (4). MCT3 is uniquely expressed in the retinal pigment epithelium. MCT1 and MCT4, but not MCT2, have been shown to interact specifically with CD147, which supports MCT expression on the cell surface. MCT1 is present in almost all tissues, whereas MCT2 is expressed in fewer tissue types, suggesting a unique functional role of this protein (6). MCT2 displays strong cytoplasmic expression, but no membrane expression in cancer (7). Experimental evidence of the presence of MCT2 in the mitochondrial membrane indicates a role in the mitochondrial import of pyruvate following lactic acid oxidation (4). Healthy colonocytes derive 60% to 70% of their energy supply from short-chain fatty acids, particularly butyrate, which is transported across the luminal membrane of the colonic epithelium via MCT1. Therefore, inhibition of MCT1 can retard tumor growth through blocking the energy supply (3). Pinheiro and colleagues reported increased expression of MCTs 1, 2, and 4 in colorectal carcinomas (8). However, earlier analysis of healthy colonic tissues and carcinomas revealed a significant decline in MCT1 protein expression during transition from normality to malignancy (9).

Irreversible cell-cycle arrest or senescence is an inherent tumor suppressive mechanism and is a critical determinant for chemotherapy. We show here that MCT2

Authors' Affiliations: [1]Biomedical Research Institute, and [2]Department of Medicine, Samsung Medical Center, Sungkyunkwan University School of Medicine, Gangnam-Gu, Seoul, Korea

Note: Supplementary data for this article are available at Molecular Cancer Therapeutics Online (http://mct.aacrjournals.org/).

Corresponding Author: Chaehwa Park or Won Ki Kang, Department of Medicine, Samsung Medical Center, Sungkyunkwan University School of Medicine, 50 Irwon-Dong, Gangnam-Gu, Seoul 135-710, Korea. Phone: 82-2-3410-3458; Fax: 82-2-3410-1757; E-mail: cpark@skku.edu; and Won Ki Kang; E-mail: wkkang@skku.edu

doi: 10.1158/1535-7163.MCT-12-0488

is selectively inhibited in DNA damage-induced cellular senescence. Moreover, protein levels of MCT2, but not MCT1, are significantly increased in colorectal carcinomas, compared with those of normal tissues. However, the effects and precise mechanisms of MCT2 inhibition in colorectal cancer remain unknown at present. 5-Fluorouracil (5-FU) is a widely used anticancer drug to treat solid tumors, including colorectal cancers. Currently, there is no effective treatment of KRAS mutated metastatic colorectal cancer, which does not respond to 5-FU combined with irinotecan or oxaliplatin chemotherapy (6). We wondered whether modulation of MCT2 might enhance sensitivity of colorectal cancer to 5-FU in KRAS mutant colorectal cancer cell lines.

In the present study, we investigated the effects of MCT2 knockdown in regulating 5-FU sensitivity of colorectal cancer. Our results showed that increased levels of reactive oxygen species (ROS) mainly mediate MCT2 knockdown, causing an increase in mitochondrial dysfunction and senescence-associated nuclear markers, including promyelocytic leukemia (PML) bodies, γH2AX, and SAHF (10). The antioxidant N-acetylcysteine (NAC), a ROS inhibitor, effectively prevented the cellular changes induced by knockdown of MCT2, supporting the involvement of ROS in this pathway. Specifically, we investigated the effects of MCT2 knockdown alone or in combination with 5-FU on human colorectal cancer xenografted in mice. The selective expression of MCT2 (but not MCT1) protein in human primary colorectal tumors, but not normal tissues, further suggests that targeting MCT2 represents a promising strategy to enhance therapeutic efficacy.

Materials and Methods

Cell culture and reagents

Human colon carcinoma (LoVo, HT29, HCT8, HCT116, SW480, and DLD1) and gastric carcinoma (MKN45 and MKN74) cells were grown in RPMI-1640 medium (Gibco Life Science) supplemented with 10% FBS, 1 mmol/L Na_2CO_3, 2 mmol/L L-glutamine, and penicillin-streptomycin. Cells were cultured at 37°C in a humidified 5% CO_2 environment. Following informed consent and in accordance with the appropriate Institutional Review Boards, tumor specimens were obtained from patients undergoing surgery at the Samsung Medical Center. The 21-nucleotide-long siRNAs targeting MCT1, MCT2, and negative control siRNA (siC) were purchased from Dharmacon. The full-length MCT2 open reading frame was obtained from LoVo mRNA using a reverse transcription-PCR (RT-PCR)-based cloning technique, and inserted into the pEGFP plasmid (Clontech). The level of ectopic MCT2 expression in stable cell lines was analyzed by immunoblotting using an anti-GFP antibody (Santa Cruz). Cells were transfected with siRNA or plasmids using Effectene (Qiagen) or an Amaxa electroporation system (Amaxa), according to the manufacturers' instructions.

RNA interference and transfection

Cells (2×10^5 cells per 60 mm dishes) were transfected with 20 nM siRNAs (Dharmacon, Lafayette, CO) using Effectene transfection reagents (Qiagen) according to the manufacturer's instructions and were used for immunoblot analysis 48 hours after transfection. Sequences of the siRNAs used were control nontargeting siRNA (5′-UAGCGACUAAACACAUCAA-3′), MCT1-targeted siRNA (siMCT1) (5′- CCAAGGCAGGGAAAGAUAAGUCUAA-3′) and MCT2-targeted siRNA (siMCT2) (5′-GGAUUUAACUGGAGAAUAU-3′).

RT-PCR

Total cellular RNA was extracted using RNeasy Mini Kit (Qiagen) and treated with DNase I (Qiagen). One microgram of RNA was converted to cDNA using Omniscript RT Kit (Qiagen). The primer sequences designed from the coding region of human MCT2 cDNA are as follows: forward, 5′- AGGATTAATTGCAAACTCCA -3′, and reverse, 5′- CCGAATGTTTAGATTTGCTC-3′. The PCR conditions were as follows: 25 cycles of 95°C for 30 seconds, 55°C for 30 seconds, and 72°C for 30 seconds, followed by a final incubation at 72°C for 10 minutes.

Senescence-associated β-galactosidase staining

Cells were seeded into 60-mm dishes in RPMI-1640 culture medium and transfected with siRNA (20 nmol/L), and senescence-associated β-galactosidase (SA-β-Gal) staining was conducted as previously described (6). Senescence was scored based on the percentage of the population that exhibited a SA-β-Gal activity, and the results were photographed under phase contrast microscopy.

Western blot analyses

Total cell extracts were obtained using lysis buffer containing 50 mmol/L Tris-HCl (pH 8.0), 150 mmol/L NaCl, 0.1% SDS, 1% NP40, and 1X protease inhibitors (Roche Applied Science), and protein concentration was determined using the micro-BCA protein reagent (Pierce). Primary antibodies against the following proteins were used: MCT1 (Sigma, AV43841, 1:1,000), MCT2 (Santa Cruz, H-40, sc-50322, 1:500), p21 (Santa Cruz, C-19, sc-397, 1:1,000), p27 (Santa Cruz, C-19, sc-528, 1:1,000), Rb (BD Pharmingen, G3-245, 554136, 1:1,000), hypophosphorylated Rb (BD Pharmingen, G99-549, 554164, 1:1,000), E2F-1 (Santa Cruz, KH95, sc-251, 1:1,000), cyclin A (Santa Cruz, H-432, sc-751, 1:1,000), Cdc2 (Santa Cruz, 17, sc-54, 1:1,000), GFP (Santa Cruz, B-2, sc-9996, 1:1,000), and β-actin (Sigma, AC-15, A5441, 1:5,000).

Assays for cell proliferation and colony formation assay

To measure cell growth *in vitro*, cells were grown in RPMI-1640 medium with 10% FBS at 37°C. Cells were seeded (1×10^5 cells per well) in a 6-well plate (Nunc) and incubated at 37°C for 1 day (24 hours). Cells were then transfected with siRNA for an additional 24 hours. Cells

were then treated with 0.25% trypsin–EDTA solution (2.5 g/L of trypsin, 0.38 g/L of EDTA; Invitrogen), stained with 0.4% trypan blue solution (Sigma-Aldrich, Inc.), and counted using a hemocytometer (Hausser Scientific). The results were expressed as percentage cell proliferation, using the number of living cells incubated with PBS as a 100% reference. For anchorage-dependent colony formation, we used DLD1, HCT8, and LoVo cells. In brief, 2×10^2 cells per well were seeded in 6-well plates (Nunc) and treated with 0.03 μg/mL 5-FU for 3 days. Triplicate cultures of each cell type were maintained at 37°C for 14 days in an atmosphere of 5% CO_2, with fresh medium being added after 7 days. Cells were stained with 0.1% (weight/vol) crystal violet.

Colonies, defined as groups of cells containing a minimum of 50 cells, were counted under an inverted phase contrast microscope. The percentage relative cell proliferation was expressed as (number of colonies from treated cells/number of colonies from controls) × 100. The assay was repeated 3 times with duplicate samples.

Cell-cycle analysis

For cell-cycle analysis, cells were washed twice with ice-cold PBS, and then fixed in 2 mL of 70% ethanol. The fixed cells were centrifuged at 200 × g for 10 minutes, and pellets were washed twice with PBS. Cells were then incubated concurrently with 40 μg/mL propidium iodide (Sigma) and 100 μg/mL RNase at 37°C for 30 minutes. The percentages of cells in different phases of the cell cycle were measured with a FAC-Star flow cytometer (BD Sciences) and analyzed using Becton-Dickinson software (CellQuest, BD Sciences).

Determination of mitochondrial mass, mitochondrial membrane potential, ROS level, and ATP concentration

LoVo cells (2×10^5 cells per well) were seeded in 6-well plates and incubated at 37°C for 1 day (24 hours). Cells were then transfected with siRNA (20 nmol/L) for an additional 5 days. To measure mitochondrial mass, Mitotracker Red (M7512; Invitrogen) was used. Cells were incubated for 5 minutes with 1 μmol/L Mitotracker Red and the intensity of labeling was measured by

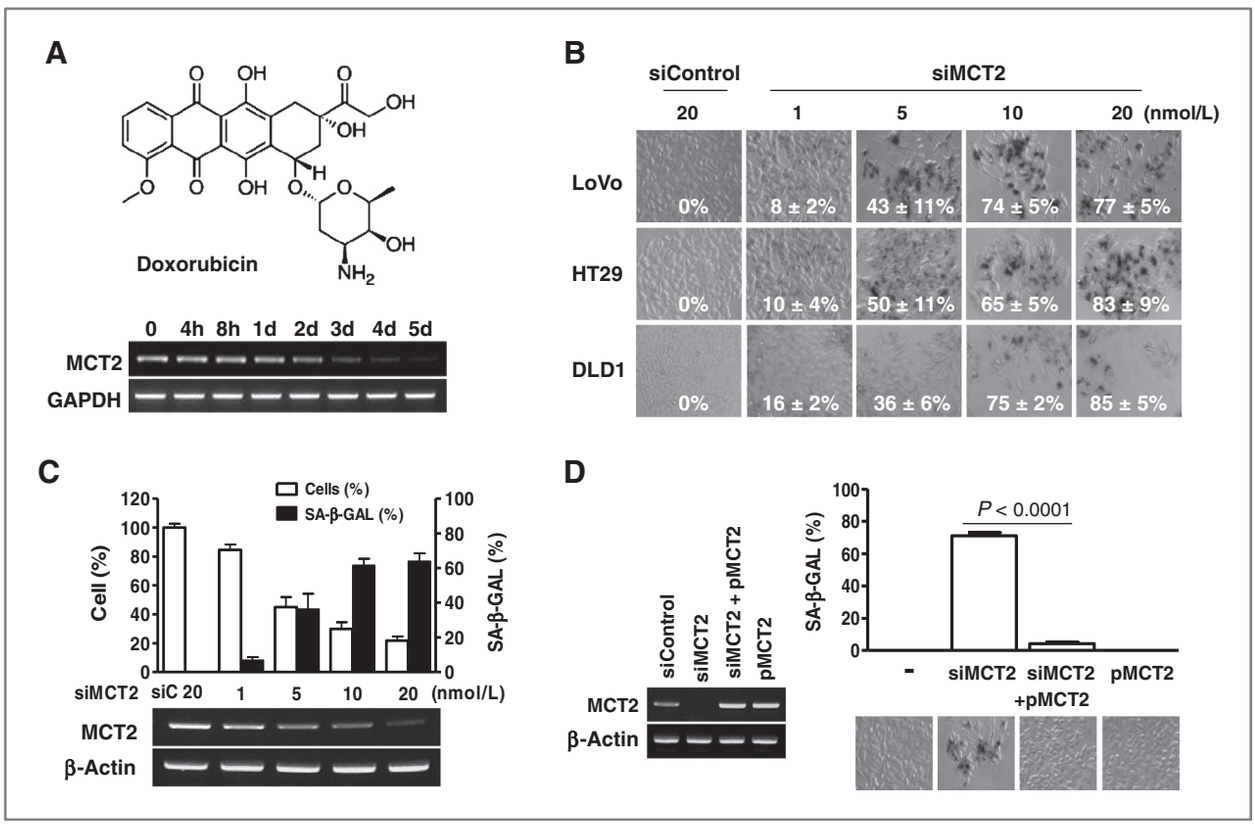

Figure 1. MCT2 is a senescence-associated molecular marker. A, RT-PCR analysis of MCT2 in doxorubicin (10 nmol/L)-treated LoVo cells. GAPDH, glyceraldehyde-3-phosphate dehydrogenase. B, siMCT2 concentration-dependent induction of senescence during colorectal cancer cell growth. C, siMCT2 concentration-dependent inhibition of LoVo cell growth. Expression of MCT2 in LoVo cells after transfection of siRNAs was examined using RT-PCR. Cell percentage, viable cell number in test sample/viable cell number in control sample × 100. The number on the right indicates the percentage of SA-β-Gal-positive cells. After culturing for 5 days, cells were stained for SA-β-Gal. D, exogenous expression of MCT2 (pMCT2) rescued cells from siMCT2-induced senescence. Cells were stained for SA-β-Gal activity 5 days after transfection.

fluorescence-activated cell sorting (FACS). To assess mitochondrial membrane potential, JC-1 (Molecular Probes) was used; cells were incubated with 10 μg/mL JC-1 for 10 minutes and washed with Hank's Buffered Salt Solution (Gibco). To measure intracellular production of ROS, we used 2 different fluorogenic probes, DCFH-DA and MitoSox (Molecular Probes). DCFH-DA reacts quantitatively with intracellular radicals, being converted to a fluorescent product, 2′,7′-dichlorofluorescein (DCF). Hydroethidine assay (11) and MitoSox were used to measure mitochondrial superoxide production. Stained cells were washed, resuspended in PBS, and analyzed using a FACS Calibur flow cytometer (BD Sciences). The ATP concentration was determined using an ATP assay kit (FL-ASC; Sigma) and the ATP/AMP ratio measured as described previously (12); data were normalized to cell number.

Immunofluorescence staining of γH2AX, PML, and SAHF

Cells were fixed in 3.7% (v/v) paraformaldehyde for 15 minutes, washed with PBS, and permeabilized using 0.2% (v/v) Triton X-100 in PBS. After blocking with 3% (w/v) bovine serum albumin (BSA) for 30 minutes, the cells were incubated for 1 hour with either anti-γH2AX (1:200; Upstate Technology) or anti-PML (1:200; Santa Cruz) in 3% (w/v) BSA in PBS. Subsequently, cells were washed 3 times with 3% (w/v) BSA in PBS and incubated with Alexa Fluor 488-conjugated secondary antibody (1:5,000) for 1 hour. 4′,6-diamidino-2-phenylindole was added to stain nuclei.

Tumorigenesis of xenotransplanted human colorectal cancer cells

Male BALB/c nude mice, 4 to 6 weeks old, were obtained from Orient Bio Inc. Mice ($n = 5$ per cell line per treatment group) were implanted subcutaneously with DLD1 (3.0×10^6 cells) in 100 μL volume using a 26-gauge needle. Each mouse received 2 subcutaneous injections in the bilateral flank for the development of 2 tumors (10 tumors per treatment group). One week after implantation, mice ($n = 5$ mice per treatment group) were assigned into 4 groups—siControl, 5-FU, siMCT2, or a combination of 5-FU and siMCT2. The mice were treated twice per week with intraperitoneal injection of 30 mg/kg 5-FU in PBS and/or once weekly intratumorally with 1 μg siMCT2 dissolved in effectene reagent. Tumor diameters were serially measured with a digital caliper (Mitutoyo) every 2 to 3 days, and tumor volumes were calculated using the following formula: $V = (L \times W^2)/2$, where V = volume (cubic millimeter), L = length (millimeter), and W = width (millimeter). The mice were killed by CO_2 inhalation, and the tumors were resected on day 15. Mice were handled at the institute's (Samsung Medical Center, Seoul, Korea) animal facility, and all treatments were in accordance with institutional guidelines.

Statistical analysis

Data presented in graphs represent means ± standard deviations of values from at least 3 independent measurements. Differences between 2 mean values were analyzed using Student t test (paired 2-sample t test). All P values less than 0.05 were considered to be statistically significant.

Results

MCT2 expression decreases according to DNA damage-induced senescence of cancer cells

Doxorubicin, a DNA damage-inducing drug frequently used to treat various types of solid tumors, triggers

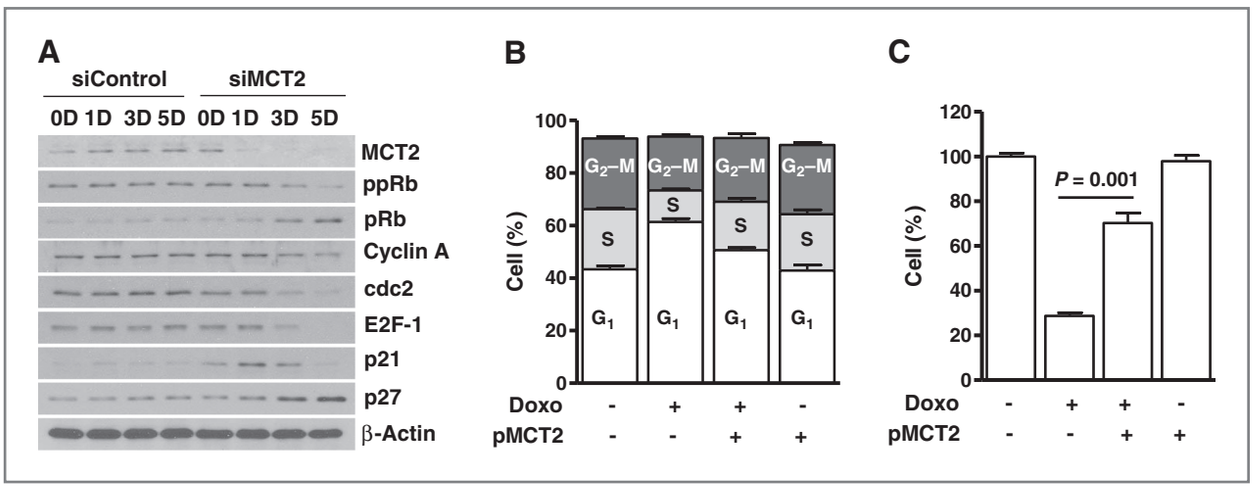

Figure 2. MCT2 knockdown induces cell-cycle arrest and senescence in colon cancer cells. A, changes in the expression of cell cycle-related proteins following siRNA transfection. LoVo cells (2×10^5 cells/well in 6-well) were seeded before siRNA transfection and harvested at the indicated times. Cell lysates containing 20 μg of protein were analyzed with SDS-PAGE/Western blotting using the antibodies shown on the right. B, rescue of doxorubicin-induced cell-cycle arrest by MCT2 overexpression. MCT2- or vector-transfected LoVo cells were treated with doxorubicin (10 nmol/L) for 5 days, fixed with 70% ethanol, and incubated with RNase A and the DNA-intercalating dye, propidium iodide. Values represent mean ± SD (bars) of 3 independent experiments. C, rescue of doxorubicin-induced growth inhibition by MCT2 overexpression. MCT2- or vector-transfected cells were treated with doxorubicin (10 nmol/L) for 5 days. Values represent the mean of 3 independent experiments.

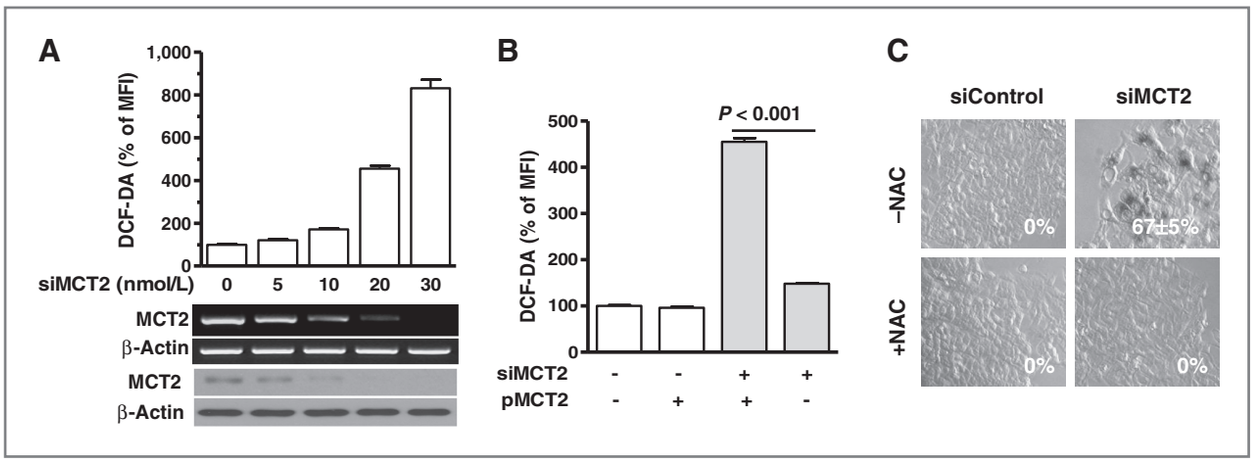

Figure 3. MCT2 knockdown induces senescence by increasing ROS accumulation. A, siMCT2 concentration-dependent increase in ROS accumulation of LoVo cells. DCF fluorescence (fold) indicates ROS generation. B, overexpression of MCT2 dramatically suppressed ROS generation induced by MCT2 knockdown ($P < 0.0001$) or doxorubicin ($P = 0.0002$). ROS levels were analyzed using the fluorescent dye DCF-DA 5 days after transfection with siRNA (20 nmol/L) or treatment of doxorubicin (10 nmol/L). MFI, mean fluorescence intensity. C, the antioxidant, NAC (10 mmol/L), blocked siMCT2-induced senescence. LoVo cells were stained for SA-β-Gal 5 days after siRNA transfection (20 nmol/L). The number indicates the percentage of SA-β-Gal-positive cells.

premature senescence (13). Low-dose doxorubicin induces growth arrest in human carcinoma cells, as evident from their SA-β-Gal positivity and flat, enlarged morphology (14, 15). In our experiments, MCT2 expression was reduced in response to doxorubicin treatment to an increasing extent with the progression of senescence (Fig. 1A). To establish whether MCT2 is directly involved in drug-induced senescence of colorectal cancer cells, we further examined the effects of MCT2 knockdown using specific siRNA (siMCT2). The growth of several cancer cells was specifically inhibited by siMCT2 (Fig. 1B), but not siMCT1 (Supplementary Fig. S1), in a concentration-

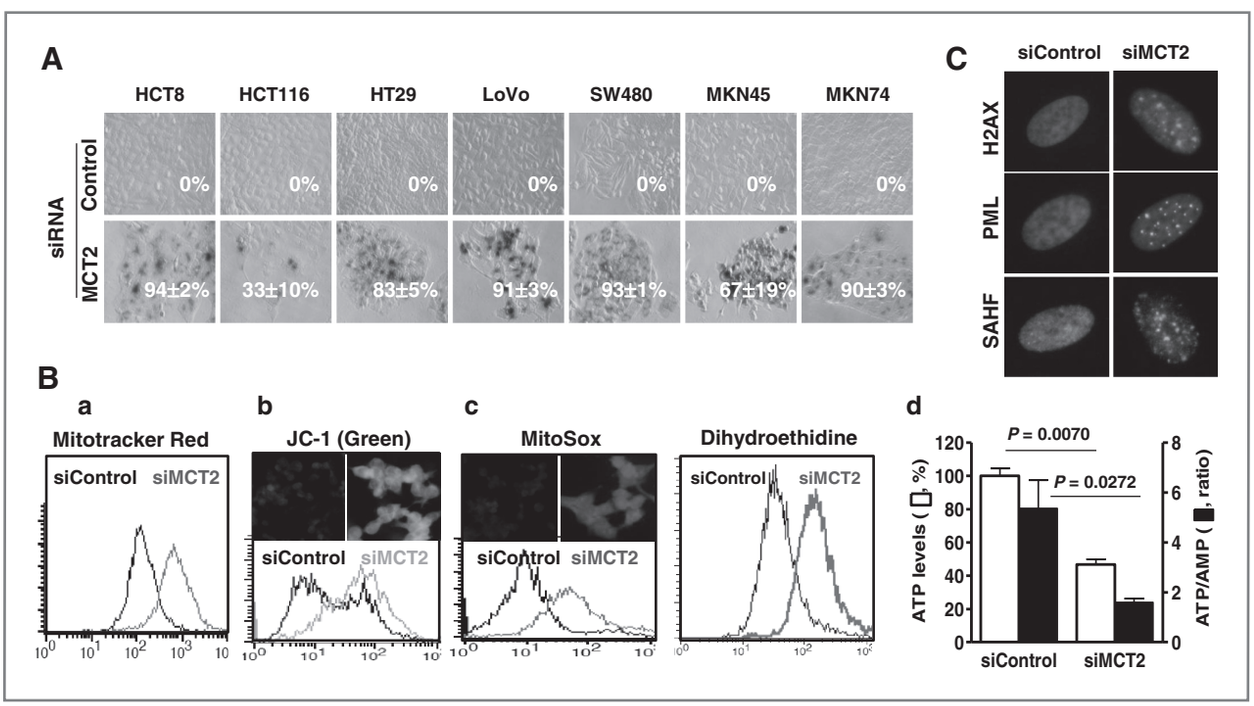

Figure 4. siMCT2 induces senescence in multiple cancer cell lines. A, HCT8, HCT116, HT29, LoVo, and SW480 and stomach (MKN45 and MKN74) cells were stained for SA-β-Gal 5 days after siRNA transfection (20 nmol/L). B, induction of senescence-associated markers after transfection of LoVo cells with the indicated siRNAs (20 nmol/L). siC, siControl. B, a, fluorescence of cells observed using flow cytometry after staining with MitoTracker Red, which permits estimation of the mitochondrial mass within cells. B, b, JC-1 fluorescence. An increase in green fluorescence indicated mitochondrial membrane depolarization. B, c, MitoSox and dihydroethidine fluorescence; indicators of mitochondrial superoxide level and therefore a measure of mitochondrial ROS. B, d, ATP content and ATP/AMP ratio in whole cells. C, immunofluorescence of γH2AX, SAHF or PML bodies.

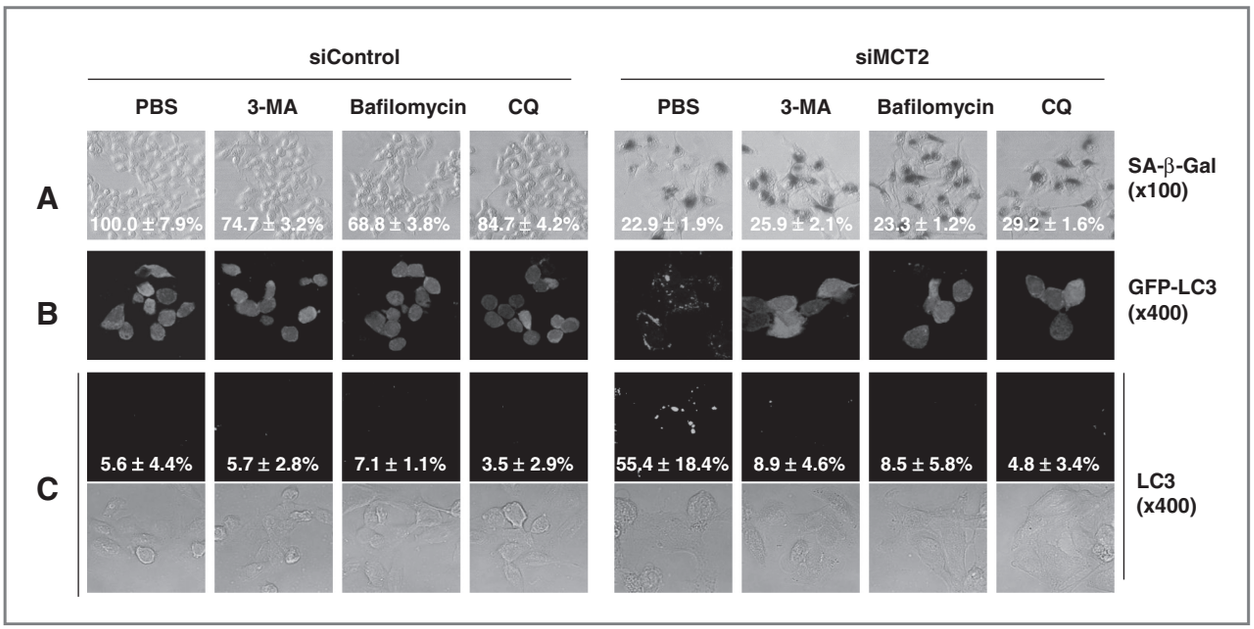

Figure 5. MCT2 knockdown triggers autophagy, but this process fails to protect cells from senescence. LoVo cells were transfected with siRNAs (20 nmol/L; MCT2 and control) in the presence or absence of the autophagy inhibitors, 3-MA (0.2 mmol/L), bafilomycin (10 nmol/L), and chloroquine (CQ, 10 μmol/L). Cells were harvested 4 days after transfection and assessed for autophagy and senescence. A, SA-β-Gal staining was conducted to estimate senescence. The number at the bottom indicates the percentage of viable cells: viable cell number in test sample/viable cell number in control (siControl, PBS) sample × 100. B, LoVo cells were cotransfected with GFP-LC3 and respective siRNAs in the presence or absence of each autophagy inhibitor. GFP-LC3 expression in cells was examined using fluorescence microscopy to detect translocation of LC3 from the cytosol to autophagic vacuoles. C, cells were stained for autophagolysosome with Cyto-ID Green Detection Reagent (Enzo Life Sciences) and observed using fluorescence and phase-contrast microscopy. The number indicates the percentage of autophagolysosome-positive cells.

dependent manner. Analysis of transfected cells revealed a siMCT2-specific decrease in MCT2 mRNA (Fig. 1C), indicative of successful knockdown. This cell growth inhibition was dose-dependent. As shown in Fig. 1D, MCT2 overexpression effectively rescued cells from siMCT2-induced senescence, clearly indicating that these biologic changes are mediated by MCT2.

ROS are involved in MCT2-modulated cell-cycle arrest

Irreversible growth arrest is associated with cell-cycle inhibitors, including p53, pRb, and the cyclin-dependent kinase inhibitors, p21, p27, and p16 (16–18). Accordingly, we investigated the effects of MCT2 knockdown on the levels of cell cycle proteins in KRAS mutated LoVo ($KRAS^{G13D}$) cells. MCT2 knockdown led to increased levels of the G1 arrest-inducing protein, p27, and decreased cdc2 and E2F1 levels and Rb phosphorylation (Fig. 2A). Next, we attempted to determine whether MCT2 overexpression suppresses cell cycle arrest and premature senescence in DNA damage-induced colorectal carcinoma cells. As shown in Fig. 2, doxorubicin-treated colorectal carcinoma cells overexpressing MCT2 exhibited decreased G_1 arrest (Fig. 2B) and improved survival (Fig. 2C), compared with doxorubicin-treated control LoVo cells.

ROS accumulation has been reported to induce senescence (10, 19). Accordingly, we investigated whether MCT2 knockdown induces ROS generation. A fluorescent marker of cellular oxidant production, DCFH-DA (20), was used to measure the intracellular levels of ROS in LoVo cells. MCT2 knockdown resulted in dramatic ROS accumulation comparing with MCT1 knockdown (Fig. 3A and Supplementary Fig. S2). Rescue of MCT2 levels via overexpression restored siMCT2-induced ROS to levels comparable to those in controls ($P < 0.0001$), indicating that accumulation of ROS is directly dependent on the MCT2 level (Fig. 3B, gray). Inhibition of ROS accumulation was previously shown to protect against senescence (21). Thus, we used the ROS scavenger, NAC (22), to determine whether accumulation of ROS plays a role in MCT2 knockdown-induced senescence. As shown in Fig. 3C, preincubation with 10 mmol/L NAC prevented senescence in MCT2 knockdown cells, indicating that senescence is induced as a consequence of ROS accumulation.

MCT2 knockdown induces senescence-associated phenotypes in mitochondria and nucleus

To ascertain whether MCT2 knockdown-induced senescence is a general phenomenon, we evaluated the senescence-inducing potential of siMCT2 in several colorectal cancer cell lines (Fig. 4A). All the cancer cell lines examined, including those of the colon (HCT8, HCT116, HT29, LoVo, and SW480) and stomach (MKN45 and MKN74), displayed cellular enlargement

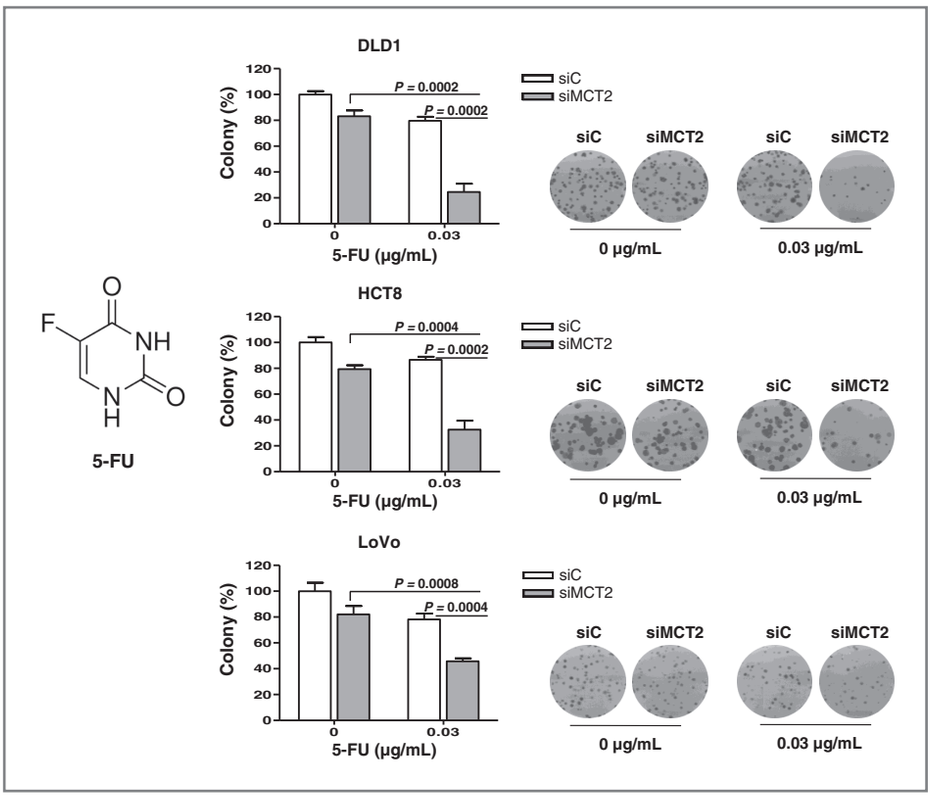

Figure 6. Colony formation assay of colorectal cancer cells. Cells (200 cells/well in 6-well) were treated with 5 nmol/L siMCT2 and/or 0.03 μg/mL 5-FU for 3 days and maintained at 37°C for 14 days, with fresh medium added after 7 days. Cells were stained with 0.1% crystal violet. *P* values are shown for 5-FU versus siMCT2+5-FU. Results are presented as means and 95% confidence intervals of 2 independent experiments conducted in quadruplicate. All *P* values were calculated using the Student *t* test.

and flattening as well as positivity for SA-β-Gal staining, following knockdown of MCT2. Moreover, depletion of MCT2, but not MCT1, resulted in mitochondrial dysfunction (23), as evident from increased mitochondrial mass (Fig. 4B, a and Supplementary Fig. S3), mitochondrial membrane potential (Fig. 4B, b), elevated mitochondrial ROS production (Fig. 4B, c), and dramatic decrease in the ATP level (Fig. 4B, d). Cells additionally exhibited senescence-associated nuclear properties, including elevation of PML bodies, γH2AX, and SAHF (Fig. 4C).

Autophagy is often induced as a survival pathway to tolerate metabolic stress. To determine whether autophagy is triggered during siMCT2-induced senescence, we evaluated autophagolysosome formation and GFP-LC3 translocation, in addition to SA-β-Gal staining. Accumulation of autophagic vacuoles was detected via fluorescence microscopic observation of GFP-LC3 translocation and Cyto-ID-stained autophagolysosomes. MCT2 knockdown cells presented green punctate structures, indicative of autophagy induction (Fig. 5). To further establish whether autophagy has a protective or toxic effect on siMCT2-transfected LoVo cells, we analyzed the outcomes of autophagy inhibition. Addition of various autophagy inhibitors (3-MA, bafilomycin, and chloroquine) led to the efficient blockage of siMCT2-induced autophagosome formation, but had no significant effects on senescence or survival of siMCT2-transfected cells.

Combined antitumor effects of MCT2 knockdown and 5-FU on colorectal cancer cells *in vitro*

In view of the above results, we speculated that MCT2 knockdown may enhance the antitumor effect of 5-FU in colon cancer. An anchorage-dependent colony formation assay was conducted to assess antitumor activity. Knockdown of MCT2 to 0.03 μg/mL 5-FU led to significant enhancement of inhibition of tumor cell colony formation in DLD1, HCT8, and LoVo cells (DLD1, 0.03 μg/mL 5-FU vs. 0.03 μg/mL 5-FU + siMCT2, $P = 0.0002$; HCT8, 0.03 μg/mL 5-FU vs. 0.03 μg/mL 5-FU + siMCT2, $P = 0.0002$; LoVo, 0.03 μg/mL 5-FU vs. 0.03 μg/mL 5-FU + siMCT2, $P = 0.0004$; Fig. 6). Clearly, a combination of 0.03 μg/mL 5-FU and siMCT2 has a greater inhibitory effect on cell growth, compared with 5-FU or siMCT2 as single agents. Our findings suggest that siMCT2 sensitizes cancer cells to 5-FU.

Effect of MCT2 on growth of colorectal tumors *in vivo*

For unknown reason, we failed to make xenotransplant tumors in mice with LoVo ($KRAS^{G13D}$) cells. Therefore, to determine whether MCT2 knockdown also has an antitumor effect *in vivo*, we implanted DLD1 ($KRAS^{G13D}$) tumors in mice and assigned the animals to 4 groups ($n = 5$ mice per treatment group), specifically, siControl, siMCT2, 5-FU, and a combination of 5-FU and siMCT2 (Fig. 7A). Knockdown of MCT2 significantly reduced tumor volume, compared with siControl ($P = 0.0264$). A combination of 5-FU and siMCT2 induced a more significant reduction in tumor volume, compared with

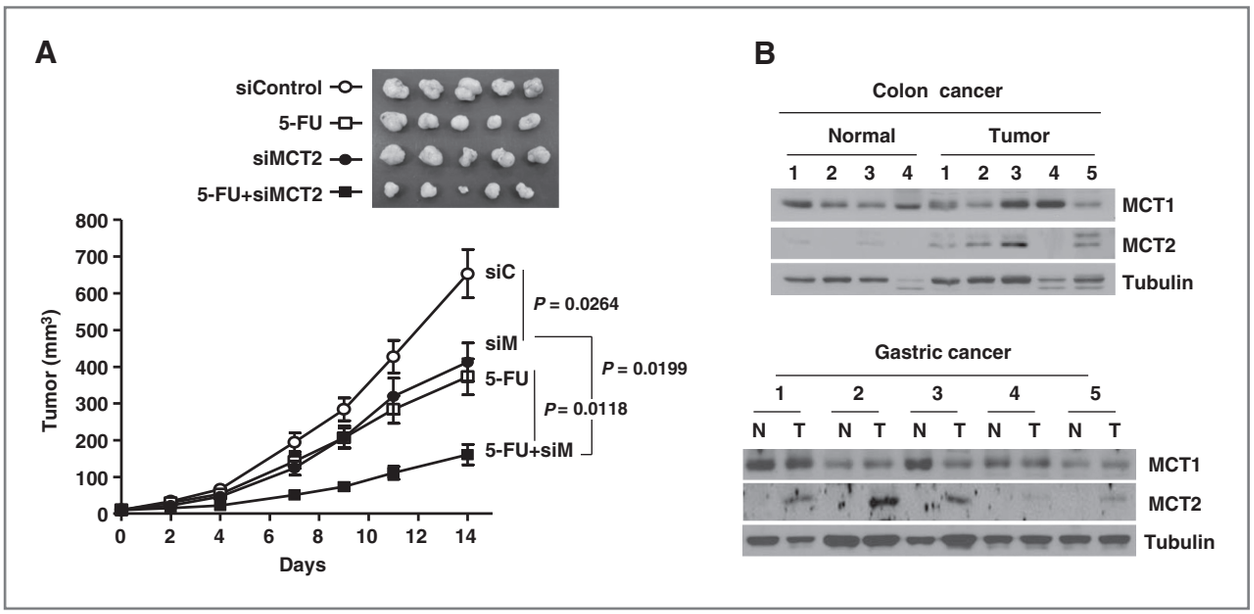

Figure 7. MCT2 expression correlates with tumorigenesis. A, MCT2 knockdown decreases *in vivo* tumorigenesis. BALB/c nude mice were injected subcutaneously in the bilateral flank (2 injections per mouse) with DLD1 cells. One week after injection, mice (5 mice and 10 tumors per treatment group) were assigned into 4 groups, specifically, siControl, siMCT2, 5-FU, and siMCT2+5-FU. Mice were treated twice per week with an intraperitoneal injection of 30 mg/kg 5-FU and/or once weekly intratumorally with 1 μg siMCT2 in effectene reagent. Tumor diameters were measured every 2 to 3 days with a digital caliper. A graphical representation of tumor volumes on different days after treatment is shown. The error bars represent 95% confidence intervals of the mean volume. *P* values were calculated using Student *t* test. Representative DLD1 xenograft tumors resected on day 15 (5 tumors per group) showing the difference in tumor volumes. B, MCT2 level is increased in human tumors. Western blot analysis of MCT1 and MCT2 in human tissues. Freshly frozen specimens of colon and gastric tumors (T) show increased MCT2 expression compared with corresponding normal tissues (N). Tubulin was used as a loading control.

5-FU ($P = 0.0118$) or siMCT2 ($P = 0.0199$) xenografts (Fig. 7B). Thus, it appears that MCT2 knockdown suppresses tumorigenicity and enhances the antitumor effect of 5-FU in colorectal cancer *in vivo*. MCT1 has additionally been implicated in tumor growth in cervix squamous carcinoma (3). Accordingly, we examined the levels of MCT1 and MCT2 in human colon and gastric cancer specimens (Fig. 7). Tumor-specific increases in MCT2, but not MCT1, were observed using Western blot analysis.

Discussion

In this study, we have shown that knockdown of MCT2 significantly suppresses the growth of cancer cells and enhances the antitumor activity of 5-FU in colorectal cancer cells. In a mouse model, growth of human colorectal xenograft tumors was significantly inhibited upon knockdown of MCT2, which was further suppressed in combination with 5-FU. To our knowledge, this is the first study to report a potential role of MCT2 as a molecular target in colorectal cancer. Previous studies of MCT2 expression in colorectal tumor samples have focused on the use of immunohistochemistry, and these studies have noted changes in the cellular location of MCT2 protein in tumor samples. Differently from MCT1 or MCT4, the immunostaining pattern of MCT2 was cytoplasmic (7, 8). Experimental evidence of the presence of MCT2 in the mitochondrial membrane indicates its role in the mitochondria (4).

Permanent growth arrest or senescence is considered an important determinant of treatment outcomes in cancer therapy (24–27). Our experiments showed that MCT2 knockdown alone induces a senescence-like phenotype in a variety of cancer cell lines, including those established from the colon (HCT8, HCT116, HT29, DLD1, and LoVo) and stomach (MKN45 and MKN74). MCT2 knockdown showed a senescence-associated mitochondrial dysfunction (23), including increases in mitochondrial mass and ROS production and decreases in the ATP level and mitochondrial membrane potential. These cells also displayed other nuclear phenotypes, including increased PML bodies (6), DNA damage-associated γH2AX foci (7), and SAHF (8).

Because MCT2 downregulation induces ROS accumulation in LoVo cells, we hypothesized that ROS is a critical mediator of MCT2 knockdown-induced senescence. ROS is a critical mediator in the induction of senescence (20, 28–30). The antioxidant, NAC, blocked ROS accumulation in response to MCT2 knockdown and protected cells from irreversible growth arrest. Therefore, we show here for the first time that ROS accumulation in response to MCT2 knockdown is responsible for causing mitochondrial dysfunction, cell-cycle arrest, and senescence.

Cellular senescence or irreversible growth arrest is associated with induction of tumor suppressors, such as p53, pRb, p16, p21, and p27 (16–18). These tumor

suppressors act through triggering ROS accumulation, which, in turn, induces permanent growth arrest/senescence (21). Therefore, induction of cell-cycle inhibitory tumor suppressors and accumulation of ROS may both contribute to irreversible growth arrest/senescence induced by MCT2 knockdown. Moreover, we found that cells displaying increased MCT2 expression are resistant to growth arrest and able to proliferate in the presence of the DNA-damaging agent, doxorubicin, that normally induces senescence. MCT1 has been previously implicated in colon (8) and cervical cancer (3). However, this is the first study showing that MCT2 is selectively overexpressed in colorectal tumors, but not MCT1. This finding is particularly significant, and supports the theory that MCT2 plays a role in escape from senescence-associated inherent tumor suppressor mechanism in colorectal cancer progression *in vivo*.

Disclosure of Potential Conflicts of Interest

No potential conflicts of interest were disclosed.

Authors' Contributions

Conception and design: W.K. Kang, C. Park
Development of methodology: I. Lee, W.K. Kang, C. Park
Acquisition of data (provided animals, acquired and managed patients, provided facilities, etc.): I. Lee, S.J. Lee, W.K. Kang, C. Park
Analysis and interpretation of data (e.g., statistical analysis, biostatistics, computational analysis): I. Lee, W.K. Kang, C. Park
Writing, review, and/or revision of the manuscript: W.K. Kang, C. Park
Administrative, technical, or material support (i.e., reporting or organizing data, constructing databases): W.K. Kang, C. Park
Study supervision: W.K. Kang, C. Park

Acknowledgments

The authors thank Prof. Kyeong Sook Choi for advice and support on autophagy experiment.

Grant Support

This work was supported by grants from IN-SUNG Foundation (CA98641) to W.K. Kang and National Research Foundation of Korea (NRF-2011-0016973) to C. Park.

The costs of publication of this article were defrayed in part by the payment of page charges. This article must therefore be hereby marked *advertisement* in accordance with 18 U.S.C. Section 1734 solely to indicate this fact.

Received May 15, 2012; revised September 4, 2012; accepted September 4, 2012; published OnlineFirst September 10, 2012.

References

1. Dewhirst MW. Mechanisms underlying hypoxia development in tumors. Adv Exp Med Biol 2003;510:51–6.
2. Dang CV, Semenza GL. Oncogenic alterations of metabolism. Trends Biochem Sci 1999;24:68–72.
3. Sonveaux P, Végran F, Schroeder T, Wergin MC, Verrax J, Rabbani ZN, et al. Targeting lactate-fueled respiration selectively kills hypoxic tumor cells in mice. J Clin Invest 2008;118:3930–42.
4. Halestrap AP, Price NT. The proton-linked monocarboxylate transporter (MCT) family: structure, function and regulation. Biochem J 1999;343:281–99.
5. Halestrap AP, Meredith D. The SLC16 gene family-from monocarboxylate transporters (MCTs) to aromatic amino acid transporters and beyond. Pflugers Arch 2004;447:619–28.
6. Christine KG, Michael SB, Ravindra KP, Joseph LG. cDNA Cloning of MCT2, a second monocarboxylate transporter expressed in different cells than MCT1. J Biol Chem 1995;270:1843–9.
7. Koukourakis MI, Giatromanolaki A, Harris AL, Sivridis E. Comparison of metabolic pathways between cancer cells and stromal cells in colorectal carcinomas: a metabolic survival role for tumor-associated stroma. Cancer Res 2006;66:632–7.
8. Pinheiro C, Longatto-Filho A, Scapulatempo C, Ferreira L, Martins S, Pellerin L, et al. Increased expression of monocarboxylate transporters 1, 2, and 4 in colorectal carcinomas. Virchows Arch 2008;452:139–46.
9. Lambert DW, Wood IS, Ellis A, Shirazi-Beechey SP. Molecular changes in the expression of human colonic nutrient transporters during the transition from normality to malignancy. Br J Cancer 2002;86:1262–9.
10. Lee I, Park C, Kang WK. Knockdown of inwardly rectifying potassium channel Kir2.2 suppresses tumorigenesis by inducing reactive oxygen species-mediated cellular senescence. Mol Cancer Ther 2010;9:2951–9.
11. Sirangelo I, Iannuzzi C, Vilasi S, Irace G, Giuberti G, Misso G, , et al. W7FW14F apomyoglobin amyloid aggregates-mediated apoptosis is due to oxidative stress and AKT inactivation caused by Ras and Rac. J Cell Physiol 2009;221:412–23.
12. Gorman MW, Marble DR, Ogimoto K, Feigl EO. Measurement of adenine nucleotides in plasma. Luminescence 2003;18:173–81.
13. te Poele RH, Okorokov AL, Jardine L, Cummings J, Joel SP. DNA damage is able to induce senescence in tumor cells *in vitro* and *in vivo*. Cancer Res 2002;62:1876–83.
14. Park C, Lee I, Kang WK. Influence of small interfering RNA corresponding to ets homologous factor on senescence-associated modulation of prostate carcinogenesis. Mol Cancer Ther 2006;5:3191–6.
15. Lee I, Yeom S-Y, Lee S, Kang WK, Park C. A novel senescence-evasion mechanism involving Grap2 and cyclin D interacting protein inactivation by Ras associated with diabetes in cancer cells under doxorubicin treatment. Cancer Res 2010;70:1–9.
16. Chang BD, Xuan Y, Broude EV. Role of p53 and p21waf1/cip1 in senescence-like terminal proliferation arrest induced in human tumor cells by chemotherapeutic drugs. Oncogene 1999;18:4808–18.
17. Hara E, Smith R, Parry D, Tahara H, Stone S, Peters G. Regulation of p16CDKN2 expression and its implications for cell immortalization and senescence. Mol Cell Biol 1996;16:859–67.
18. Alexander K, Hinds PW. Requirement for p27(KIP1) in retinoblastoma protein-mediated senescence. Mol Cell Biol 2001;21:3616–31.
19. Chen Q, Ann F, Joshua DR, Yan L-J, Bruce NA. Oxidative DNA damage and senescence of human diploid fibroblast cells. Proc Natl Acad Sci U S A 1995;92:4337–41.
20. Royall JA, Ischiropoulos H. Evaluation of 2′,7′-dichlorofluorescin and dihydrorhodamine 123 as fluorescent probes for intracellular H_2O_2 in cultured endothelial cells. Arch Biochem Biophys 1993;302:348–55.
21. Macip S, Igarashi M, Fang L, Chen A, Pan ZQ, Lee SW, et al. Inhibition of p21-mediated ROS accumulation can rescue p21-induced senescence. Embo J 2002;21:2180–8.
22. Staal FJ, Roederer M, Herzenberg LA. Intracellular thiols regulate activation of nuclear factor kappa B and transcription of human immunodeficiency virus. Proc Natl Acad Sci U S A 1990;87:9943–7.
23. Moiseeva O, Bourdeau V, Roux A, Deschênes-Simard X, Ferbeyre G. Mitochondrial dysfunction contributes to oncogene-induced senescence. Mol Cell Biol 2009;29:4495–507.
24. Schmitt CA, Fridman JS, Yang M, Lee S, Baranov E, Hoffman RM, et al. A senescence program controlled by p53 and p16INK4a contributes to the outcome of cancer therapy. Cell 2002;109:335–46.
25. Roninson IB. Tumor cell senescence in cancer treatment. Cancer Res 2003;63:2705–15.

26. Chang BD, Broude EV, Dokmanovic M, Zhu H, Ruth A, Xuan Y, et al. A senescence-like phenotype distinguishes tumor cells that undergo terminal proliferation arrest after exposure to anticancer agents. Cancer Res 1999;59:3761–7.

27. Gewirtz DA, Holt SE, Elmore LW. Accelerated senescence: an emerging role in tumor cell response to chemotherapy and radiation. Biochem Pharmacol 2008;76:947–57.

28. Ames BN, Shigenaga MK, Hagen TM. Oxidants, antioxidants, and the degenerative diseases of aging. Proc Natl Acad Sci U S A 1993;90:7915–22.

29. Beckman KB, Ames BN. The free radical theory of aging matures. Physiol Rev 1998;78:547–81.

30. Finkel T, Holbrook NJ. Oxidants, oxidative stress and the biology of ageing. Nature 2000;408:239–47.